

---

# RoboFail: Analyzing Failures in Robot Learning Policies

---

**Som Sagar**  
Arizona State University  
ssagar6@asu.edu

**Ransalu Senanayake**  
Arizona State University  
ransalu@asu.edu

## Abstract

Despite being trained on increasingly large datasets, robot models often overfit to specific environments or datasets. Consequently, they excel within their training distribution but face challenges in generalizing to novel or unforeseen scenarios. This paper presents a method to proactively identify failure mode probabilities in robot manipulation policies, providing insights into where these models are likely to falter. To this end, since exhaustively searching over a large space of failures is infeasible, we propose a deep reinforcement learning-based framework, RoboFail. It is designed to detect scenarios prone to failure and quantify their likelihood, thus offering a structured approach to anticipate failures. By identifying these high-risk states in advance, RoboFail enables researchers and engineers to better understand the robustness limits of robot policies, contributing to the development of safer and more adaptable robotic systems.

## 1 Introduction

Robotic systems are increasingly deployed in complex and dynamic environments where adaptability and resilience to unexpected conditions are critical. While advancements in machine learning, particularly in reinforcement learning [1] and large-scale data-driven training [2, 3, 4], have enabled robots to perform a wide array of tasks. Models trained on extensive datasets [5] or optimized based on specific parameter configurations frequently excel within their training distributions but may struggle when exposed to novel or unanticipated situations. Such limitations in generalization not only constrain the reliability of robotic policies but also raise safety concerns in real-world applications, where failures can lead to significant operational or even safety-critical issues.

This paper introduces RoboFail, a deep reinforcement learning-based framework developed to proactively identify potential failure mode (FM) [6] in robotic policies. Rather than addressing overfitting directly, RoboFail focuses on mapping high-risk scenarios in advance, where robotic policies are likely to falter. By evaluating FM probabilities, the framework provides a structured approach for assessing the robustness of robotic models and identifying specific conditions that could lead to failure. This probabilistic analysis enables a deeper understanding of the inherent vulnerabilities in robotic policies, contributing to the development of systems that are both safer and more resilient to unexpected challenges.

RoboFail operates by simulating diverse conditions and systematically quantifying the likelihood of policy failure in each scenario. The framework’s probabilistic approach offers insights into failure-prone states, allowing researchers and engineers to anticipate and prepare for potential breakdowns before deploying robotic systems in real-world settings. Ultimately, RoboFail supports the creation of robotic policies that are not only reliable within their training bounds but also adaptable across a wide range of operational contexts, thus enhancing both their safety and applicability. The approach comprises of three main key components: environment design, reinforcement learning setup, and FM analysis.

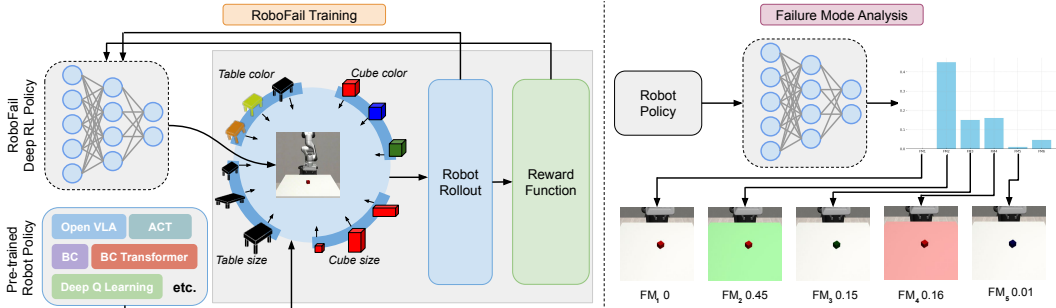


Figure 1: RoboFail Framework: (1) Pre-trained robot policy undergoes rollouts while controlled perturbations (P) simulate diverse scenarios. A PPO-based reinforcement learning agent identifies configurations most likely to induce failures; (2) Once PPO training is complete, the agent’s output distribution, given an observation, is analyzed to derive probabilities for each failure mode (FM), quantifying the likelihood of failure.

## 2 Related Work

One of the ways to understand the failures in robot learning models is through the eyes of uncertainty. Characterizing aleatoric uncertainty—the known unknowns—through probabilistic models is ubiquitous in classical robotic systems [7]. On the other hand, while many attempts have been made to characterize the epistemic uncertainty—the unknown unknowns—in robot perception systems [8, 9], only a few addresses this challenge in deep reinforcement learning [10, 11] and imitation learning [12, 13, 14]. [15] provides an overview of aleatoric and epistemic uncertainty quantification methods in robot learning systems.

As robot policies grow increasingly complex, formally characterizing uncertainty becomes challenging. An alternative for this is searching for areas where the model fails. This can be done by utilizing the general knowledge of vision-language foundation models [16, 17, 18, 19], learning an expert failure prediction model [6], or a combination of both [20]. For this purpose, outside of robotics, deep reinforcement learning has recently been employed in machine learning to effectively identify and mitigate the failures such as image misclassification, text summarization errors, and bias in image generation [6, 20] as well as in regression models [21]. [22, 23] utilized RL to explore adversarial scenarios and stress test model robustness. [24] highlights the role of sequential decision making models in ensuring the safety of black-box systems. Considering the dynamic nature of robot manipulation, in this work, we explore using deep RL to analyze failure modes of robot manipulation policies.

Failures are particularly likely to occur when operating outside the training distribution. Out-of-distribution (OOD) detection methods have been extensively studied to address the challenge of robots encountering data outside their training distributions. For example, Nitsch et al. [25] proposed OOD detection methods for automotive perception without requiring additional training or inference costs. Similarly, Wilson et al. [26] introduced sensitivity-aware features to enhance OOD object detection performance. Tools such as PyTorch-OOD have further streamlined the evaluation and implementation of OOD detection methods [27]. Our objective is to characterize failures both within and outside the training distribution.

Another premise is that generalized robots are less prone to failures. Towards achieving this goal, generalization in robotics has been extensively studied to enable robots to adapt to diverse and unforeseen scenarios. Large-scale simulation frameworks have been developed to evaluate the robustness of robotic policies across varied tasks and environmental conditions [28]. Vision-language-action models trained on multimodal datasets have demonstrated significant advancements in improving adaptability to real-world scenarios [2, 3]. Additionally, approaches such as curriculum learning and domain randomization have proven effective in enhancing generalization by exposing models to progressively complex or randomized environments [29]. These methodologies collectively address the challenges of simulation-to-reality transfer and robustness, providing foundational insights that complement RoboFail’s targeted failure mode identification for improving policy generalization.

There are numerous other work on characterizing safety from a controls theory perspective [30, 31], human factors perspective [32], etc. Work on providing theoretical certificates through statistical methods [33, 34, 35, 36] or formal methods [37] are also highly valuable. These diverse approaches to solving the problem collectively contribute to more robust and safer robot deployment.

### 3 RoboFail

RoboFail employs a reinforcement learning-based approach, to identify and quantify FM’s in robotic policies. Through systematic environment modifications and probabilistic analysis, RoboFail reveals conditions that challenge policy robustness and generalization. The following methodology outlines our approach in three stages: action-driven environment manipulation, failure learning, and probabilistic analysis of FM’s.

**Action-driven environment manipulation:** To systematically explore potential FM’s, we designed an environment where an agent can manipulate specific attributes of the robotic simulation. The environment is based on a robotic manipulation task using the robomimic [38] which provides a flexible platform for experimentation. In this environment, the agent has the ability to perform discrete actions that modify environmental parameters. Each action corresponds to a specific manipulation by allowing the agent to directly influence the environment, we enable a targeted exploration of scenarios that may induce policy failures.

**Failure discovery:** The core of RoboFail’s approach to identifying FM’s lies in the use of reinforcement learning, specifically Proximal Policy Optimization (PPO) [39], to train an agent that seeks out environmental configurations leading to policy failures. The agent’s policy network is parameterized by a convolutional neural network (CNN) to process visual observations and output action probabilities. The value function is trained concurrently to estimate the expected return from each state, aiding in policy updates.

#### 3.1 Reinforcement Learning

**Motivation:** RL offers a systematic approach to exploring the action space by optimizing the selection of actions based on their potential to induce failures. Unlike heuristic or uniform sampling methods, RL adapts action selection dynamically, enabling targeted exploration of high-risk configurations and maximizing the efficiency of failure mode identification. For a detailed rationale behind choosing RL for this framework, see Appendix C.

We formulate the failure discovery process as a Markov Decision Process (MDP) defined by the tuple  $\langle \mathcal{S}, \mathcal{A}, \mathcal{P}, R, \gamma \rangle$ , here the agent’s goal is to maximize the occurrence of failures in the manipulation policy. In this setup, the agent interacts with the environment in discrete time steps, aiming to maximize the cumulative reward. For this task, the objective is to train the agent to maximize the occurrence of failures in a policy, effectively exploring high-risk states that challenge the robustness of the policy. Unlike a naive for-loop that uniformly samples all 20 actions, reinforcement learning leverages an optimization framework to dynamically allocate selection probabilities based on the likelihood of failure. By learning a policy tailored to identify high-risk scenarios, RL enables efficient exploration of the action space, prioritizing configurations that are most informative for failure mode analysis.

##### 3.1.1 Setup

The components of the RL setup are:

1. State Space ( $\mathcal{S}$ ): The state is represented by the current observation from the environment, including visual data of the robot and workspace after the agent’s action has been applied.
2. Action Space ( $\mathcal{A}$ ): A discrete set of actions allowing the agent to modify environmental parameters.
3. Reward Function ( $R$ ): The reward function is designed to encourage the discovery of failure scenarios while penalizing successful task completions based on the time taken. The agent is rewarded positively when the policy under test fails to complete the task, and negatively

when the task is successfully completed, with the penalty scaled by the task duration.

$$R = \begin{cases} 1000 & \text{if the policy fails to complete the task,} \\ \frac{-100}{\text{horizon}} & \text{if the policy succeeds.} \end{cases} \quad (1)$$

4. Transition Dynamics ( $\mathcal{P}(s'|s, a)$ ): The transition dynamics define the probability of transitioning from one state ( $s$ ) to another ( $s'$ ) after taking an action ( $a$ ). In this context, the dynamics are dictated by the physics engine of the robotic environment, introducing stochasticity through environmental noise, uncertainty in robot behavior, or other external factors. This stochastic modeling ensures realistic variability in state transitions.
5. Discount Factor ( $\gamma$ ): The discount factor  $\gamma \in [0, 1]$  determines the weight of future rewards relative to immediate rewards. In our setup, we set  $\gamma = 0.99$ , which prioritizes long-term planning while maintaining sufficient sensitivity to immediate outcomes.

### 3.1.2 Proximal Policy Optimization

We employ PPO as the learning algorithm for the agent due to its effectiveness in handling large action spaces and high-dimensional observations. PPO optimizes the policy by performing multiple epochs of stochastic gradient ascent on a surrogate objective function, which is clipped to prevent excessively large policy updates that could destabilize training. The PPO objective function is defined as:

$$L^{\text{CLIP}}(\theta) = \mathbb{E}_t \left[ \min \left( r_t(\theta) \hat{A}_t, \text{clip} \left( r_t(\theta), 1 - \epsilon, 1 + \epsilon \right) \hat{A}_t \right) \right], \quad (2)$$

where:

- $r_t(\theta) = \frac{\pi_\theta(a_t|s_t)}{\pi_{\theta_{\text{old}}}(a_t|s_t)}$  is the probability ratio,
- $\hat{A}_t$  is the estimated advantage function,
- $\epsilon$  is the clipping parameter to control the deviation from the old policy  $\pi_{\theta_{\text{old}}}$ ,
- $\min$  ensures that the objective does not grow unbounded, maintaining stability during updates.

The agent’s policy network is parameterized by a convolutional neural network (CNN) to process visual observations  $s_t$  and output action probabilities  $\pi_\theta(a_t | s_t)$ , detailed specifications of the CNN architecture are provided in Appendix B.. The value function, parameterized by a separate network or shared with the policy network, is trained concurrently to minimize the following loss:

$$L^{\text{VF}}(\theta_v) = \mathbb{E}_t \left[ (V_{\theta_v}(s_t) - R_t)^2 \right], \quad (3)$$

where:

- $V_{\theta_v}(s_t)$  is the value function estimating the expected return from state  $s_t$ ,
- $R_t = \sum_{k=0}^{\infty} \gamma^k r_{t+k}$  is the discounted return.

During training, the agent selects an action  $a_t \sim \pi_\theta(a | s_t)$  to modify the environment based on its current policy. The environment applies the modification, and the policy under test attempts to complete its task in the new configuration. The reward  $r_t$  is received by the agent based on the success or failure of the policy under test, with the total loss combining the policy and value function losses:

$$L(\theta) = L^{\text{CLIP}}(\theta) - c_1 L^{\text{VF}}(\theta_v) + c_2 H(\pi_\theta), \quad (4)$$

where:

- $H(\pi_\theta)$  is the entropy regularization term to encourage exploration,
- $c_1$  and  $c_2$  are coefficients to balance the value function loss and entropy term.

The specific hyperparameters used for training PPO are detailed in Appendix A.

This process repeats for a predefined number of episodes or until convergence. By incentivizing the agent to find configurations where the policy under test fails, PPO enables targeted exploration of the failure space while maintaining training stability and efficiency.

## 4 Analyzing Failure Modes

Understanding FM’s in robotic policies is essential for improving their robustness and reliability. By examining the likelihood of each action under specific observations, we can systematically identify and rank vulnerabilities in the policy.

To quantify FM’s in robotic policies, we analyze the probability distribution over actions generated by the trained RL agent’s policy. This distribution highlights actions that are most likely to induce failure conditions, providing a probabilistic framework for identifying critical vulnerabilities in the policy under test.

After training the RL agent with PPO, we obtain a policy  $\pi_\theta(a | s)$ , which maps a state  $s$  with observation  $o$  to a probability distribution over the action space  $\mathcal{A}$ . For a given observation  $o_i$ , the policy’s log probability of selecting an action  $a$  is computed as:

$$\log \pi_\theta(a | o_i) = f_\theta(o_i)_a - \log \left( \sum_{a' \in \mathcal{A}} \exp(f_\theta(o_i)_{a'}) \right) \quad (5)$$

where:

- $f_\theta(o_i)_a$  represents the unnormalized logit (score) for action  $a$ ,
- $\sum_{a' \in \mathcal{A}} \exp(f_\theta(o_i)_{a'})$  is the normalization term ensuring that the probabilities sum to 1.

Using the log probabilities, we derive the policy’s probability distribution over actions via the softmax function:

$$\pi_\theta(a | o_i) = \frac{\exp(f_\theta(o_i)_a)}{\sum_{a' \in \mathcal{A}} \exp(f_\theta(o_i)_{a'})} \quad (6)$$

The resulting policy distribution  $\pi_\theta(a | o_i)$  reflects the likelihood of each action  $a$  under the current observation  $o_i$ . We interpret this distribution as a measure of failure likelihood, with actions assigned higher probabilities considered more likely to induce failures in the policy under test.

To explicitly quantify the failure likelihood associated with a specific action  $a$ , we define:

$$P_{\text{failure}}(a) = \pi_\theta(a | o_i) \quad (7)$$

where the normalization condition holds:

$$\sum_{a \in \mathcal{A}} P_{\text{failure}}(a) = 1 \quad (8)$$

The probabilities  $P_{\text{failure}}(a)$  provide an interpretable ranking of actions, enabling us to prioritize failure modes based on their likelihood of inducing policy breakdowns. For example, in a robotic manipulation task, actions like “grasp” or “move” may have high  $P_{\text{failure}}(a)$  in specific states where the robot’s end-effector alignment or grip strength is inadequate. Such insights can guide targeted policy retraining to address these weaknesses.

## 5 Experiments

We conduct experiments to evaluate the effectiveness of RoboFail in identifying FM’s across different robot manipulation policies example shown in Fig 2, each trained with varying input modalities. Specifically, we test policies using visual (image), proprioceptive, language, and combined multi-modal inputs. This setup allows us to analyze how different sensory and contextual inputs impact policy robustness and generalization in diverse environments.

### 5.1 Experimental Setup

**Models and Input Modalities:** We evaluate multiple models trained on distinct input modalities to analyze their contributions to policy performance and susceptibility to failure. The evaluated models include:

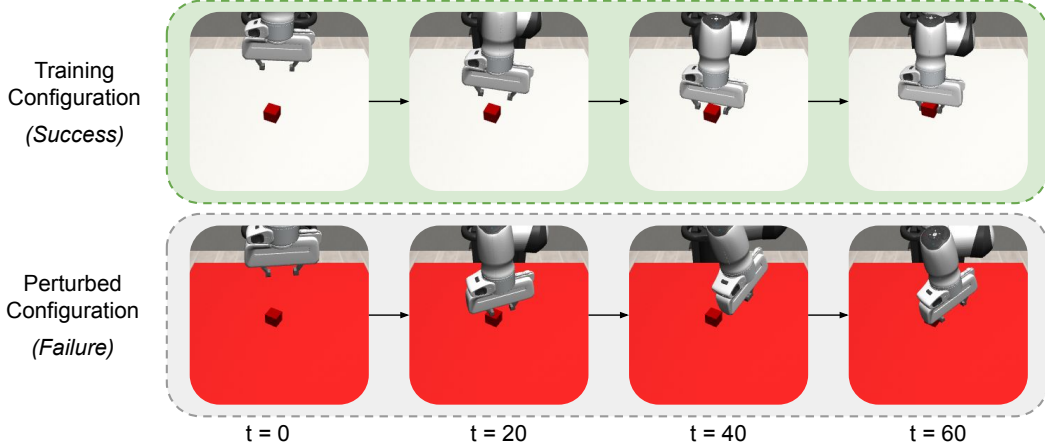


Figure 2: Testing Robustness Under Visual Perturbations: Successful Rollout in Training vs. Failure Induced by Red Table Distraction

- **Image(n) Model:** This model is trained using  $n$  RGB images as input, providing the policy with visual information about the environment.
- **Image + Proprioceptive Model:** This model relies on RGB images and proprioceptive data, which includes joint angles, positions, and other intrinsic states, representing the robot’s own sensory feedback without external visual cues.
- **Image + Language Model:** This model uses RGB images and natural language input, this model interprets task instructions and environmental descriptions with visual information.

**Task and Environment Details:** The policies are evaluated on manipulation tasks, including stacking, pushing, and reaching, within a simulated environment built on Robosuite [40].

## 5.2 Results

We test robofail in multiple models as shown in Fig 3. We see that most tasks are overfitted to perform well in the environmental setup they are trained from but small environmental perturbations cause the model to fail. We see individual model failure mapping in Fig 4.

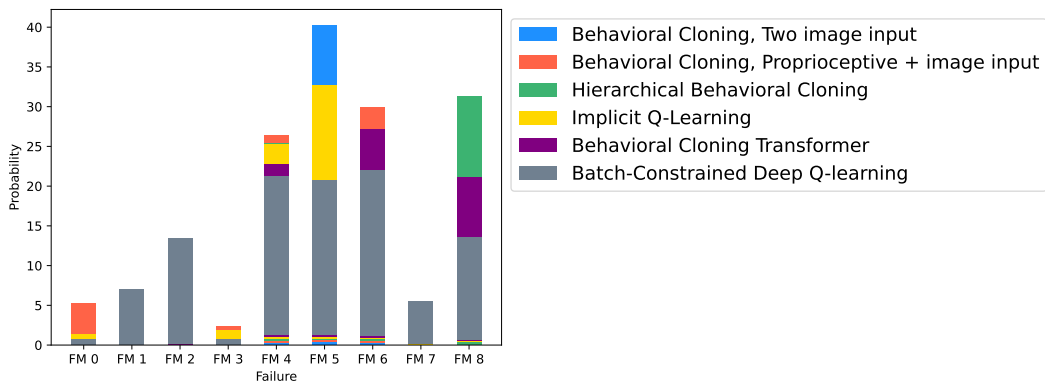


Figure 3: FM analysis of multiple models. The stacked bars illustrate the contributions of different models to each failure mode, highlighting model-specific vulnerabilities and the distribution of failure probabilities across the action space.

Fig 4 visualizes the failure mode analysis for multiple models across different environmental configurations (e.g., Red Cube, Green Table, Blue Table). Each radar plot represents the failure likelihood  $P_{\text{failure}}(a)$  for specific actions, derived using the above framework. For more analysis refer to Appendix E.

**Key Points for Interpretation:** The failure likelihood  $P_{\text{failure}}(a)$  is computed using a softmax function, meaning the probabilities are normalized across all failure modes. A low  $P_{\text{failure}}(a)$  for one mode does not necessarily imply a low probability of failure, as other failure modes may dominate the distribution. Models that fail consistently across all configurations (poor policies) may exhibit a more uniform probability distribution across failure modes. This is because softmax normalization spreads the probabilities more evenly. A high  $P_{\text{failure}}(a)$  values in certain configurations suggest that the model has specific vulnerabilities to those scenarios. For example, if  $P_{\text{failure}}(a)$  is high for the "Red Cube" environment in a specific model, it implies that the model is particularly prone to failure in that scenario. Poorly performing models are likely to exhibit nearly equal  $P_{\text{failure}}(a)$  values across all failure modes, indicating that they fail indiscriminately in multiple scenarios. For a mathematical rationale refer to Appendix D.

It is important to note that  $P_{\text{failure}}(a)$  can be interpreted as  $P(\text{Failure} | \text{Env})$ , which represents the probability of failure given the environment.

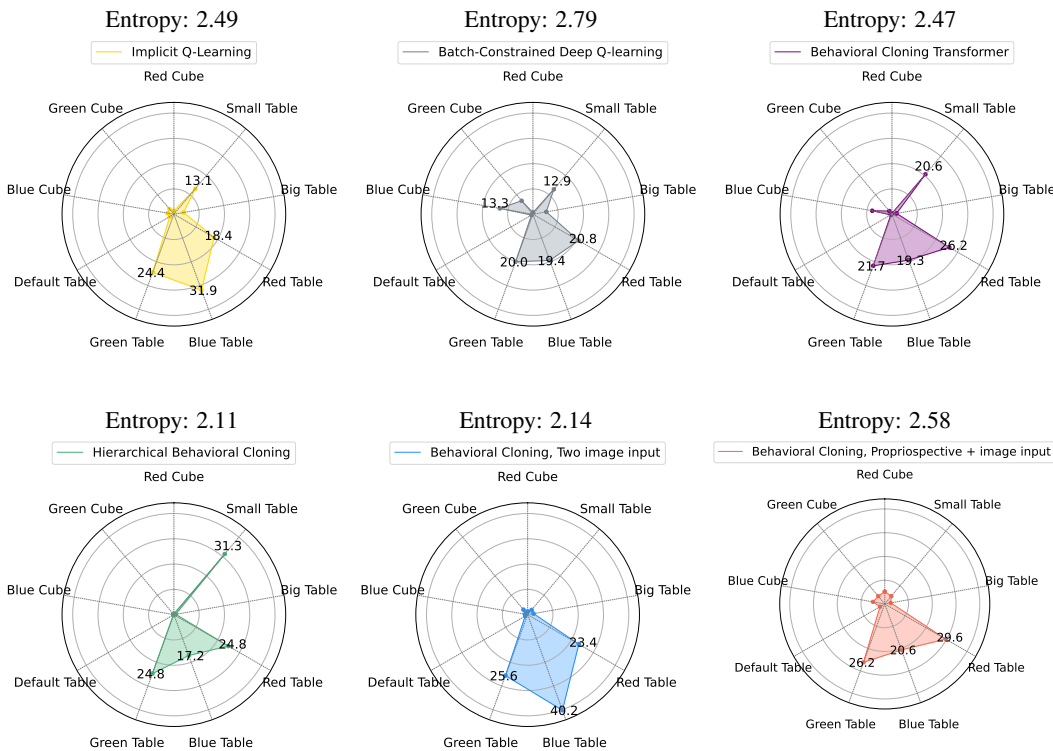


Figure 4: Individual FM analysis of multiple models. Each radar plot represents the failure likelihood  $P_{\text{failure}}(a)$  of specific actions. The axes correspond to different environmental setups (e.g., Red Cube, Green Table, Blue Table), and the numbers indicate the probability of failure for actions under each configuration. This visualization highlights the relative vulnerabilities of each model to specific failure-inducing scenarios.

Fig 4 demonstrates that higher entropy values, such as 2.79 for “Batch-Constrained Deep Q-learning,” indicate a more even distribution of failures across multiple scenarios, suggesting broader vulnerability to diverse conditions. In contrast, models with lower entropy, like “Hierarchical Behavioral Cloning” with 2.11, show concentrated failure patterns, making their issues more predictable and easier to address. This relationship between entropy and failure distribution underscores the trade-off between predictability and robustness, where higher entropy often correlates with an increased overall failure risk due to widespread susceptibility.

## 6 Conclusion

In this work, RoboFail, a deep reinforcement learning-based framework designed to systematically identify and quantify FM’s in robotic policies was introduced. By leveraging controlled environmental manipulations and probabilistic analysis, RoboFail provides a structured approach for testing policy robustness and discovering scenarios where policies are likely to fail. Through comprehensive experiments, we evaluated various models across different input modalities, including image, proprioception, language, and multimodal combinations, to understand how sensory inputs influence resilience to environmental perturbations. Future work will focus on dramatically increasing the actions space and interactions of environment conditions [20]. By proactively identifying and mitigating potential failure scenarios, RoboFail contributes to the development of safer, more reliable robotic systems capable of operating effectively in unpredictable and complex environments.

## References

- [1] Scott Fujimoto, David Meger, and Doina Precup. Off-policy deep reinforcement learning without exploration. In *International conference on machine learning*, pages 2052–2062. PMLR, 2019.
- [2] Anthony Brohan, Noah Brown, Justice Carbajal, Yevgen Chebotar, Joseph Dabis, Chelsea Finn, Keerthana Gopalakrishnan, Karol Hausman, Alex Herzog, Jasmine Hsu, et al. Rt-1: Robotics transformer for real-world control at scale. *arXiv preprint arXiv:2212.06817*, 2022.
- [3] Anthony Brohan, Noah Brown, Justice Carbajal, Yevgen Chebotar, Xi Chen, Krzysztof Chormanski, Tianli Ding, Danny Driess, Avinava Dubey, Chelsea Finn, et al. Rt-2: Vision-language-action models transfer web knowledge to robotic control. *arXiv preprint arXiv:2307.15818*, 2023.
- [4] Octo Model Team, Dibya Ghosh, Homer Walke, Karl Pertsch, Kevin Black, Oier Mees, Sudeep Dasari, Joey Hejna, Tobias Kreiman, Charles Xu, et al. Octo: An open-source generalist robot policy. *arXiv preprint arXiv:2405.12213*, 2024.
- [5] Abby O’Neill, Abdul Rehman, Abhinav Gupta, Abhiram Maddukuri, Abhishek Gupta, Abhishek Padalkar, Abraham Lee, Acorn Pooley, Agrim Gupta, Ajay Mandlekar, et al. Open x-embodiment: Robotic learning datasets and rt-x models. *arXiv preprint arXiv:2310.08864*, 2023.
- [6] Som Sagar, Aditya Taparia, and Ransalu Senanayake. Failures are fated, but can be faded: Characterizing and mitigating unwanted behaviors in large-scale vision and language models. In *Forty-first International Conference on Machine Learning*, 2024.
- [7] Sebastian Thrun. Probabilistic robotics. *Communications of the ACM*, 45(3):52–57, 2002.
- [8] Simon T O’Callaghan and Fabio T Ramos. Gaussian process occupancy maps. *The International Journal of Robotics Research*, 31(1):42–62, 2012.
- [9] Alex Kendall and Yarin Gal. What uncertainties do we need in bayesian deep learning for computer vision? *Advances in neural information processing systems*, 30, 2017.
- [10] Harrison Charpentier, Ransalu Senanayake, Mykel Kochenderfer, and Stephan Günnemann. Disentangling epistemic and aleatoric uncertainty in reinforcement learning. In *ICML 2022 Workshop on Distribution-Free Uncertainty Quantification*, 2022.
- [11] Yiding Jiang, J Zico Kolter, and Roberta Raileanu. On the importance of exploration for generalization in reinforcement learning. *Advances in Neural Information Processing Systems*, 36, 2024.
- [12] Wonseok Jeon, Seokin Seo, and Kee-Eung Kim. A bayesian approach to generative adversarial imitation learning. *Advances in neural information processing systems*, 31, 2018.
- [13] Daniel Brown, Russell Coleman, Ravi Srinivasan, and Scott Niekum. Safe imitation learning via fast bayesian reward inference from preferences. In *International Conference on Machine Learning*, pages 1165–1177. PMLR, 2020.
- [14] Deepak Ramachandran and Eyal Amir. Bayesian inverse reinforcement learning. In *IJCAI*, volume 7, pages 2586–2591, 2007.



- [15] Ransalu Senanayake. The role of predictive uncertainty and diversity in embodied ai and robot learning. *arXiv preprint arXiv:2405.03164*, 2024.
- [16] Christopher Agia, Rohan Sinha, Jingyun Yang, Zi-ang Cao, Rika Antonova, Marco Pavone, and Jeannette Bohg. Unpacking failure modes of generative policies: Runtime monitoring of consistency and progress. *arXiv preprint arXiv:2410.04640*, 2024.
- [17] Jiafei Duan, Wilbert Pumacay, Nishanth Kumar, Yi Ru Wang, Shulin Tian, Wentao Yuan, Ranjay Krishna, Dieter Fox, Ajay Mandlekar, and Yijie Guo. Aha: A vision-language-model for detecting and reasoning over failures in robotic manipulation. *arXiv preprint arXiv:2410.00371*, 2024.
- [18] Lukas Klein, Kenza Amara, Carsten T Lüth, Hendrik Strobelt, Mennatallah El-Assady, and Paul F Jaeger. Interactive semantic interventions for vlms: A human-in-the-loop investigation of vlm failure. In *Neurips Safe Generative AI Workshop 2024*.
- [19] Rakshith Subramanyam, Kowshik Thopalli, Vivek Narayanaswamy, and Jayaraman J Thiagarajan. Decider: Leveraging foundation model priors for improved model failure detection and explanation. In *European Conference on Computer Vision*, pages 465–482. Springer, 2025.
- [20] Som Sagar, Aditya Taparia, and Ransalu Senanayake. Llm-assisted red teaming of diffusion models through " failures are fated, but can be faded". *arXiv preprint arXiv:2410.16738*, 2024.
- [21] Jayaraman J Thiagarajan, Vivek Narayanaswamy, Puja Trivedi, and Rushil Anirudh. Pager: A framework for failure analysis of deep regression models. *arXiv preprint arXiv:2309.10977*, 2023.
- [22] Harrison Delecki, Masha Itkina, Bernard Lange, Ransalu Senanayake, and Mykel J Kochenderfer. How do we fail? stress testing perception in autonomous vehicles. In *2022 IEEE/RSJ International Conference on Intelligent Robots and Systems (IROS)*, pages 5139–5146. IEEE, 2022.
- [23] Zhang-Wei Hong, Idan Shenfeld, Tsun-Hsuan Wang, Yung-Sung Chuang, Aldo Pareja, James Glass, Akash Srivastava, and Pulkit Agrawal. Curiosity-driven red-teaming for large language models. *arXiv preprint arXiv:2402.19464*, 2024.
- [24] Anthony Corso, Robert Moss, Mark Koren, Ritchie Lee, and Mykel Kochenderfer. A survey of algorithms for black-box safety validation of cyber-physical systems. *Journal of Artificial Intelligence Research*, 72:377–428, 2021.
- [25] Julia Nitsch, Masha Itkina, Ransalu Senanayake, Juan Nieto, Max Schmidt, Roland Siegwart, Mykel J Kochenderfer, and Cesar Cadena. Out-of-distribution detection for automotive perception. In *2021 IEEE International Intelligent Transportation Systems Conference (ITSC)*, pages 2938–2943. IEEE, 2021.
- [26] Samuel Wilson, Tobias Fischer, Feras Dayoub, Dimity Miller, and Niko Sünderhauf. Safe: Sensitivity-aware features for out-of-distribution object detection. In *Proceedings of the IEEE/CVF International Conference on Computer Vision*, pages 23565–23576, 2023.
- [27] Konstantin Kirchheim, Marco Filax, and Frank Ortmeier. Pytorch-ood: A library for out-of-distribution detection based on pytorch. In *Proceedings of the IEEE/CVF Conference on Computer Vision and Pattern Recognition*, pages 4351–4360, 2022.
- [28] Wilbert Pumacay, Ishika Singh, Jiafei Duan, Ranjay Krishna, Jesse Thomason, and Dieter Fox. The colosseum: A benchmark for evaluating generalization for robotic manipulation. *arXiv preprint arXiv:2402.08191*, 2024.
- [29] OpenAI: Marcin Andrychowicz, Bowen Baker, Maciek Chociej, Rafal Jozefowicz, Bob McGrew, Jakub Pachocki, Arthur Petron, Matthias Plappert, Glenn Powell, Alex Ray, et al. Learning dexterous in-hand manipulation. *The International Journal of Robotics Research*, 39(1):3–20, 2020.
- [30] Andrea Bajcsy and Jaime F Fisac. Human-ai safety: A descendant of generative ai and control systems safety. *arXiv preprint arXiv:2405.09794*, 2024.
- [31] Philipp Grimmeisen, Friedrich Sautter, and Andrey Morozov. Concept: Dynamic risk assessment for ai-controlled robotic systems. *arXiv preprint arXiv:2401.14147*, 2024.
- [32] Lindsay Sanneman and Julie A Shah. The situation awareness framework for explainable ai (safe-ai) and human factors considerations for xai systems. *International Journal of Human-Computer Interaction*, 38(18-20):1772–1788, 2022.

- [33] Alec Farid, David Snyder, Allen Z Ren, and Anirudha Majumdar. Failure prediction with statistical guarantees for vision-based robot control. *arXiv preprint arXiv:2202.05894*, 2022.
- [34] Allen Z Ren and Anirudha Majumdar. Distributionally robust policy learning via adversarial environment generation. *IEEE Robotics and Automation Letters*, 7(2):1379–1386, 2022.
- [35] Heng Yang, Jingnan Shi, and Luca Carlone. Teaser: Fast and certifiable point cloud registration. *IEEE Transactions on Robotics*, 37(2):314–333, 2020.
- [36] Joseph A Vincent, Haruki Nishimura, Masha Itkina, and Mac Schwager. Full-distribution generalization bounds for imitation learning policies. In *First Workshop on Out-of-Distribution Generalization in Robotics at CoRL 2023*, 2023.
- [37] Jana Tůmová, Luis I Reyes Castro, Sertac Karaman, Emilio Frazzoli, and Daniela Rus. Minimum-violation ltl planning with conflicting specifications. In *2013 American Control Conference*, pages 200–205. IEEE, 2013.
- [38] Ajay Mandlekar, Danfei Xu, Josiah Wong, Soroush Nasiriany, Chen Wang, Rohun Kulkarni, Li Fei-Fei, Silvio Savarese, Yuke Zhu, and Roberto Martín-Martín. What matters in learning from offline human demonstrations for robot manipulation. In *Conference on Robot Learning (CoRL)*, 2021.
- [39] John Schulman, Filip Wolski, Prafulla Dhariwal, Alec Radford, and Oleg Klimov. Proximal policy optimization algorithms. *arXiv preprint arXiv:1707.06347*, 2017.
- [40] Yuke Zhu, Josiah Wong, Ajay Mandlekar, Roberto Martín-Martín, Abhishek Joshi, Soroush Nasiriany, and Yifeng Zhu. robosuite: A modular simulation framework and benchmark for robot learning. *arXiv preprint arXiv:2009.12293*, 2020.

## A PPO Hyperparameters Used for Training

The following hyperparameters were used for training PPO with a CNN policy (Appendix B):

- **Learning rate:** 0.0003,
- **Number of steps per rollout (`n_steps`):** 2048,
- **Batch size:** 64,
- **Number of epochs:** 10,
- **Discount factor ( $\gamma$ ):** 0.99,
- **Generalized Advantage Estimation ( $\lambda$ ):** 0.95,
- **Entropy coefficient (`ent_coef`):** 0.0,
- **Value function coefficient (`vf_coef`):** 0.5,
- **Max gradient norm (`max_grad_norm`):** 0.5.

## B Policy Architecture

The policy network is configured as follows:

### Feature Extractor: NatureCNN

The feature extractor processes RGB observations with the following convolutional layers:

- **Conv2D-1:** 32 filters, kernel size  $8 \times 8$ , stride 4, activation: ReLU.
- **Conv2D-2:** 64 filters, kernel size  $4 \times 4$ , stride 2, activation: ReLU.
- **Conv2D-3:** 64 filters, kernel size  $3 \times 3$ , stride 1, activation: ReLU.
- **Flatten:** The output is flattened to a 1D vector of size 3136.
- **Fully Connected Layer:** 512 units, activation: ReLU.

### Policy and Value Networks

The extracted features are passed to separate policy and value networks:

- **Policy Network (Actor):** Outputs action probabilities using a linear layer with 512 input features and 9 output units (corresponding to the action space size).
- **Value Network (Critic):** Outputs a scalar state value using a linear layer with 512 input features and 1 output unit.

This architecture effectively handles high-dimensional input data, such as RGB images, and maps them to actionable policies while concurrently estimating state values.

## C Rationale for Using Reinforcement Learning

RL is employed in the RoboFail framework due to its ability to explore high-dimensional, complex action spaces and optimize sequential decision-making under uncertainty. This section outlines the key motivations for choosing RL as the core methodology:

**Exploration of High-Risk Scenarios:** Traditional approaches to analyzing robot policy failures often rely on deterministic sampling or exhaustive evaluation, which become infeasible in large, dynamic environments. RL allows targeted exploration by learning an agent that actively seeks out environmental configurations likely to induce policy failures. This capability is particularly useful for systematically uncovering vulnerabilities in high-dimensional environments.

**Optimization of Failure Discovery:** The objective of RoboFail is to maximize the occurrence of failures in pre-trained policies. RL frameworks, such as PPO, are well-suited for this task as they

iteratively refine policies to achieve specific goals, such as identifying high-risk states. The reward function incentivizes the agent to find configurations where the policy under test fails, streamlining the failure discovery process.

**Adaptability to Dynamic Environments:** Robotic systems operate in environments characterized by uncertainty and dynamic changes. RL’s inherent ability to adapt to stochastic transition dynamics ensures that the exploration process remains robust even in the presence of environmental noise or variability. This adaptability enhances the reliability of failure mode analysis across diverse conditions. Also RL’s capacity to handle the sequential nature of decision-making, allowing the framework to focus on cohesive patterns of actions that collectively contribute to failures. By modeling sequences of actions as interconnected behaviors, RL enables a more structured and efficient exploration of failure-inducing scenarios

**Comparison with Alternative Methods:** While other methods, such as supervised learning or heuristic-based exploration, can provide valuable insights into specific failure cases, they are limited in their scope and adaptability. Supervised learning approaches rely heavily on labeled data, which is challenging to obtain for failure analysis, particularly for rare or unseen failure modes. These methods also lack the ability to adapt dynamically to changes in the environment, reducing their effectiveness in exploring novel or complex failure scenarios. Similarly, heuristic-based exploration methods, such as grid search or predefined sampling strategies, can identify failure cases under controlled conditions but struggle to generalize in high-dimensional environments where the space of possible failure configurations is vast. These methods are also constrained by their reliance on static, predefined rules, which often fail to capture the intricate interactions between environmental factors and failure likelihoods. In contrast, reinforcement learning excels in scenarios where exploration and generalization are critical. Through reward-driven learning, RL agents actively seek configurations that maximize the probability of failure, uncovering patterns and interactions that static methods are likely to miss. Moreover, RL does not require a fully labeled dataset; it iteratively refines its policy through interaction with the environment, making it highly adaptive and scalable. By focusing on cumulative rewards, RL is uniquely positioned to generalize across a wide range of failure-inducing conditions, including edge cases and scenarios resulting from complex factor interactions. This adaptability and exploratory capability make RL an ideal framework for large-scale failure analysis in dynamic and uncertain environments, surpassing the limitations of traditional supervised learning or heuristic-based approaches.

## D Mathematical Rationale for Policy Output Distributions

The probabilities  $\pi_\theta(a | o_i)$  generated by a policy are derived from the logits  $f_\theta(o_i)_a$ , which represent the unnormalized scores for each action  $a$  given an observation  $o_i$ . Using the softmax function, these logits are converted into probabilities as:

$$\pi_\theta(a | o_i) = \frac{\exp(f_\theta(o_i)_a)}{\sum_{a' \in \mathcal{A}} \exp(f_\theta(o_i)_{a'})}. \tag{9}$$

The distribution  $\pi_\theta(a | o_i)$  reflects the policy’s preference for different actions under the given state. The characteristics of this distribution depend on the variation in the logits  $f_\theta(o_i)_a$ :

- **Low Variance in Logits:** When the logits for all actions are similar (e.g.,  $f_\theta(o_i)_a \approx f_\theta(o_i)_{a'}$  for all  $a, a'$ ), the softmax output approaches a uniform distribution. This occurs in poorly trained models or in scenarios where the policy lacks sufficient information to differentiate between actions. The softmax normalization evenly distributes probabilities when the logits lack significant variation.
- **High Variance in Logits:** When the logits for some actions are significantly higher than others, the softmax output becomes skewed, with higher probabilities assigned to actions corresponding to the larger logits. This indicates that the policy has a strong preference for certain actions, reflecting effective differentiation and a clear understanding of the environment.

The softmax function ensures that the probabilities  $\pi_\theta(a | o_i)$  always sum to 1, regardless of the logits’ absolute values. This property normalizes the policy’s preferences into a probabilistic framework, allowing consistent interpretation of action probabilities.

## Implications for Failure Mode Analysis

The distribution  $\pi_{\theta}(a | o_i)$  plays a crucial role in analyzing failure modes:

- **Uniform Distribution:** A uniform  $P_{\text{failure}}(a)$  across failure modes suggests indiscriminate vulnerability, as the model is unable to prioritize specific actions or scenarios.
- **Skewed Distribution:** A skewed  $P_{\text{failure}}(a)$  indicates targeted vulnerabilities, where certain actions or scenarios are more likely to induce failures.

This rationale highlights how the underlying logits  $f_{\theta}(o_i)_a$  influence the interpretation of failure probabilities and the ability of a policy to handle diverse environmental conditions.

## E Additional Analysis

To provide an alternative visualization, we include a heatmap (Fig 5) that shows the normalized failure probabilities for each model across all environments. The rows correspond to models, while the columns represent environments. The intensity of the color indicates the magnitude of the failure probability, with darker colors representing higher probabilities.

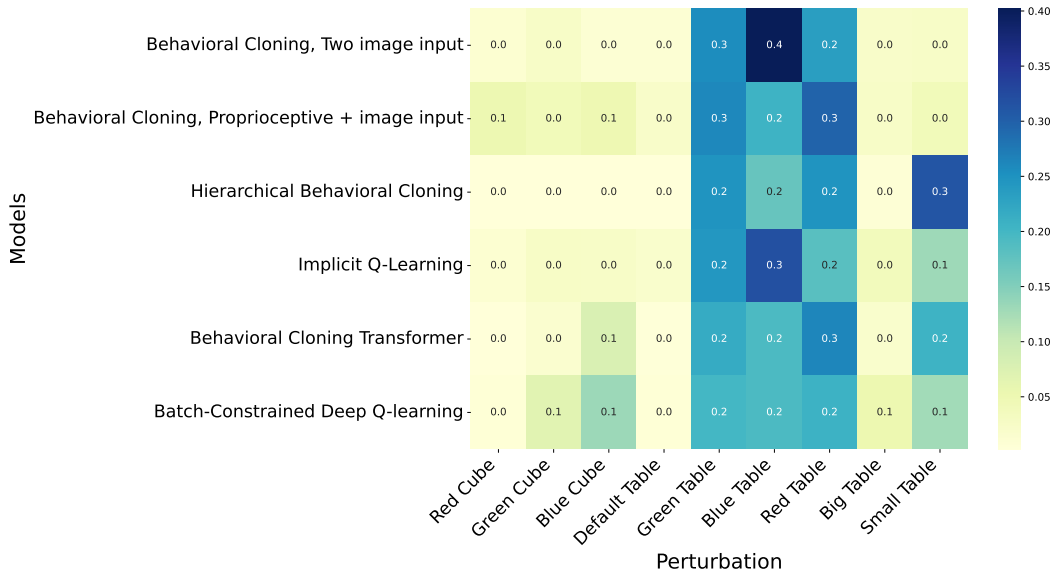


Figure 5: Heatmap of normalized failure probabilities across models and environments. This visualization highlights the environments most prone to causing failures for specific models.

Fig 6 shows the grouped bar chart where the probabilities of failure for each model are visualized across all failure modes (FM). Each bar represents the likelihood of failure for a specific model in a given failure mode, enabling direct comparison of model performance.

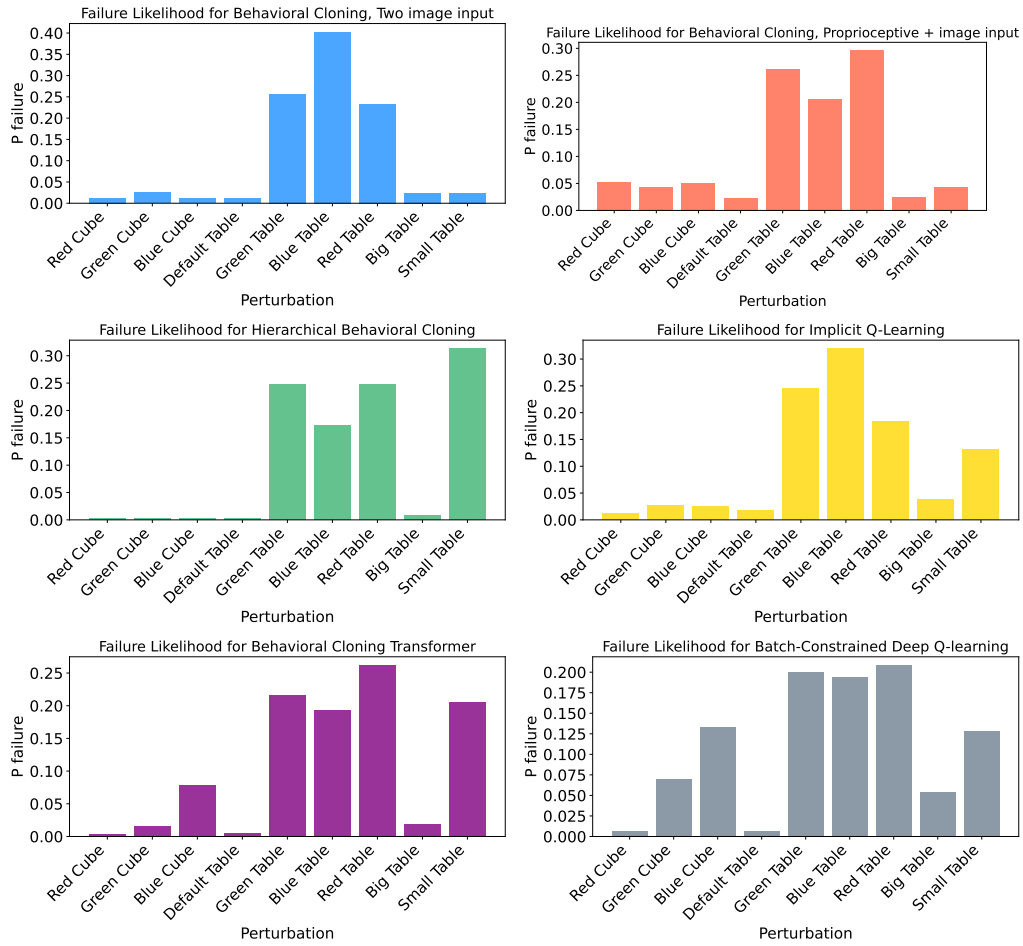


Figure 6: Bar chart showing failure probabilities for individual models across various FM. Each bar represents the likelihood of failure for a specific model under a given failure mode. This visualization provides a clear comparison of model performance and their vulnerabilities to specific failure scenarios.